

A Dialectical Approach for Classification of DW-MR Alzheimer's Images

Wellington P. dos Santos, Ricardo E. de Souza, Plínio B. Santos Filho,
Fernando B. Lima Neto, and Francisco M. de Assis

Abstract—Multispectral image analysis is a relatively promising field of research with applications in several areas, such as medical imaging and satellite monitoring. However, a considerable number of current methods of analysis are based on parametric statistics. Alternatively, some methods in Computational Intelligence are inspired by biology and other sciences. Here we claim that Philosophy can be also considered as a source of inspiration. This work proposes the Objective Dialectical Method (ODM), which is a computational intelligent method for classification based on the Philosophy of Praxis. Here, ODM is instrumental in assembling evolvable mathematical tools to analyze multispectral images. In the case study described in this paper, such multispectral images are composed of diffusion-weighted (DW) magnetic resonance (MR) images. The results are compared to ground-truth images produced by polynomial networks using a morphological similarity index.

I. INTRODUCTION

The dialectical conception of reality is a kind of philosophical investigative method for analyzing processes present in nature and in human societies. Its origins are connected to the philosophy of the ancient civilizations of Greece, China and India, closely connected to the thoughts of Heraclite, Plato, and the philosophies of Confucionism, Buddhism, and Zen. As a general analysis method, dialectics has experienced considerable progress due to the development of German Philosophy in the 19th century, with Hegel's dialectics and, in the 20th century, the works of Marx, Engels, and Gramsci. All those philosophers produced seminal works on the dynamics of contradictions in nature and class-based societies, giving rise to the Historical Materialism [1], [2], [3], [4], [5].

The dialectical method of Historical Materialism is a tool for studying systems by considering the dynamics of their contradictions, as dynamic processes with intertwined phases of *evolution* and *revolutionary crisis*. It has inspired us to conceive an evolvable computational intelligent method for classification that is able to solve problems commonly approached by neural networks and genetic algorithms.

Wellington P. dos Santos and Fernando B. Lima Neto are with Departamento de Sistemas e Computação, Escola Politécnica de Pernambuco, Universidade de Pernambuco, 50720-001, Recife, Pernambuco, Brazil (e-mail: {wps, fbln}@dsc.upe.br).

Ricardo E. de Souza is with Departamento de Física, Universidade Federal de Pernambuco, 50670-901, Recife, Pernambuco, Brazil (e-mail: res@df.ufpe.br).

Plínio B. Santos Filho is with the Department of Physics, North Carolina State University, Raleigh, North Carolina, USA (e-mail: c2511@terra.com.br).

Francisco M. de Assis is with Departamento de Engenharia Elétrica, Universidade Federal de Campina Grande, 58109-970, Campina Grande, Paraíba, Brazil (e-mail: fmarcos@dee.ufcg.edu.br).

This work was partially supported by CNPq-Brazil.

Each of the most common paradigms of Computational Intelligence, namely neural networks, evolutionary computing, and culture-inspired algorithms, has its basis in a kind of theory intended to be of general application, but in fact very incomplete; e.g. the neural networks approach is based on a certain model of the brain; evolutionary computing is based on Darwin's theory; and cultural-inspired algorithms are based on the study of populations, such as those of ant colonies. However, it is important to note that it is not necessarily the case (and indeed it may be impossible) that the theories an algorithm are based on have to be complete. For example, neural networks utilize a well-known incomplete model of the neurons. This is a strong reason for investigating the use of Philosophy as a source of inspiration for developing computational intelligent methods and models to apply in several areas, such as pattern recognition.

Thornley and Gibb discussed the application of Dialectics to understand more clearly the paradoxical and conceptually contradictory discipline of information retrieval [6], while Rosser Jr. attempted to use some aspects of Dialectics in nonlinear dynamics, comparing some aspects of Marx and Engel's dialectical method with concepts of Catastrophe Theory, Emergent Dynamics Complexity and Chaos Theory [7]. However, there are no works proposing a mathematical approach to establish the fundamentals of Dialectics as a tool for constructing computational intelligent methods.

This work introduces the Objective Dialectical Method (ODM), which is an evolvable computational intelligent method, and the Objective Dialectical Classifier (ODC), an instance of ODM that operates as a non-supervised self-organized map dedicated to pattern recognition and classification. ODM is based on the dynamics of contradictions among dialectical poles. In the task of classification, each class is considered as a dialectical pole. Such poles are involved in pole struggles and affected by revolutionary crises, when some poles may disappear or be absorbed by other ones. New poles can emerge following periods of revolutionary crisis. Such a process of pole struggle and revolutionary crisis tends to a stable system, e.g. a system corresponding to the clusterization of the original data. As a case study, we use ODC to classify magnetic resonance multispectral images as an option for improving diagnosing by imaging ¹.

¹Notice that we are not concerned whether Dialectics is a closed model, i.e. a complete theory. We are just interested in demonstrating through an important application that Dialectics can be useful for building computational intelligent models and tools, e.g. pattern classifiers.

In medical terms, Alzheimer's disease is the most common cause of dementia, both in senile and presenile individuals, experimenting the gradual course of the disease as the individual becomes older [8], [9], [10]. The major manifestation of Alzheimer's disease is the diminution of the cognitive functions with gradual loss of memory, including psychological, neurological and behavioral symptoms indicated by a decline in the performance of daily life activities as a whole [11].

Alzheimer's disease is characterized by the reduction of the gray matter near the cerebral sulci. As the gray matter is also responsible for memory, its reduction explains the gradual loss of memorization abilities in senile individuals affected by this disease. However, the white matter is also affected, although the precise relation between Alzheimer's disease and white matter damage is still unknown [12], [13], [14].

The acquisition of magnetic resonance diffusion-weighted images enables the visualization of the increase in the lateral ventriculi temporal corni, enhancing the enlargement of the sulci that is related to the worsening of the symptoms of Alzheimer's disease [15].

Therefore, the precise volumetrical measurement of cerebral structures is very important in the diagnosis and evaluation of the progression of diseases such as Alzheimer's [9], [16], [17], [18], [19], especially the measurement of areas occupied by the sulci and lateral ventriculi, because such measurement enables quantitative information to be added to the qualitative information provided by the magnetic resonance diffusion-weighted images [20].

The evaluation of the progress of Alzheimer's disease using image analysis of diffusion-weighted magnetic resonance images is performed after the acquisition of at least three images of each slice of interest, where each image is acquired by using a spin-echo sequence with different diffusion exponents. One of these diffusion exponents must be equal to 0 s/mm², that is, one of the images has to be a T₂-weighted spin-echo image [12], [15].

Using images acquired as mentioned above, a fourth image is obtained. It is referred to as an Apparent Diffusion Coefficient Map, or ADC map, in which each pixel is associated with the corresponding apparent diffusion coefficient of the associated voxel. The brighter the pixels of the ADC map, the greater the corresponding apparent diffusion coefficients [15].

Based on ODM, this paper proposes a new approach for evaluation of the progress of Alzheimer's disease. Since the ADC map usually presents pixels with considerable intensities in regions not occupied by the sample, a degree of uncertainty can also be considered in the pixels inside the sample. Furthermore, the ADC map is also sensitive to the presence of noise in images [15]. This paper approaches image analysis and classification of synthetic multispectral images composed of diffusion-weighted (DW) magnetic resonance (MR) cerebral images by using the objective dialectical classifier as an alternative to the ADC map. In

the case study presented in this paper, real images are used to compose a multispectral image, where each diffusion-weighted image is considered as an spectral band in a synthetic multispectral image. The MR images were acquired from a single volunteer with Alzheimer's, using an image system based on a clinical 1.5 T tomographer.

II. THE OBJECTIVE DIALECTICAL METHOD

The Objective Dialectical Method (ODM) is an evolvable computation intelligent method designed to model dynamic systems and to perform tasks of classification, pattern recognition, intelligent search and optimization.

General principles of ODM are as the following algorithm:

- 1) System inputs must be represented as a *vector of conditions* representing the main features of the problem;
- 2) The user has to provide the initial parameters for: *poles* or *classes* that compose the system, *number of historical phases*, and *duration of each historical phase*. The number of historical phases and their duration can also be randomly defined;
- 3) Each dialectical pole is associated with: (i) a *vector of weights*, with the same size as the vector of conditions; (ii) an *anticontradiction function*, and (iii) a *measure of force*. Such a vector of weights can be randomly defined or chosen from the set of vectors of conditions;
- 4) The historical phases consist of two stages:
 - a) **Evolution:** Where conditions are presented to the inputs of the system and the integrating poles compete with each other, in a process called *pole struggle*. Then, an anticontradiction function associated with each pole is evaluated and, given a vector of conditions, the winner pole, which is the pole with greatest anticontradiction value, has its parameters (weights and measure of force) incremented. This process continues until the end of the historical phase is reached;
 - b) **Revolutionary crisis:** This starts at the end of the historical phase. At this point the following steps are performed:
 - i) The measures of force are compared, i.e., all the poles with a measure of force less than a minimum force are marked;
 - ii) The contradictions among the integrating poles are also evaluated. If a contradiction between two poles is less than a given minimum contradiction, one of the two poles is selected or marked as such. Here the minimum contradiction plays the role of a threshold;
 - iii) From the evaluated contradictions computed in the previous items, the overall maximum contradiction is calculated. This is *the main contradiction* of the system. From the pair of poles involved in the main contradiction, a new pole is generated, i.e. a synthesis of previous pair of poles, whose vector of weights is calculated from the vector of weights of the

- pair. It is also possible to choose more than one main contradiction and, from its involved pairs of poles, generate other new poles;
- iv) All the marked poles are eliminated and a new set of integrating poles is generated;
 - v) The vector of weights of all poles of the new set of poles is randomly modified, representing the impact of the revolutionary crisis on both the survivors and the new dialectical poles.

III. OBJECTIVE DIALECTICAL CLASSIFIERS

Objective Dialectical Classifiers are based on the Objective Dialectical Method. They are an adaptation of ODM to tasks of classification. This means that the feature vectors are mounted and considered as vectors of conditions. Specifically, once they are applied to the inputs of the dialectical system, their coordinates will affect the dynamics of the contradictions among the integrating dialectical poles. Hence, the integrating poles model the recognized classes at the task of non-supervised classification.

Therefore, an objective dialectical classifier is in fact an adaptable and evolvable non-supervised classifier where, instead of supposing a predetermined number of classes, we can set an initial number of classes (dialectical poles) and, as the historical phases happen (as a result of pole struggles and revolutionary crises), some classes are eliminated, others are absorbed, and a few others are generated. At the end of the training process, the system presents a number of statistically significant classes present in the training set and, therefore, a feasible classifier associated to the final state of the dialectical system.

To accelerate the convergence of the dialectical classifier, we have removed the operator of pole generation, present at the revolutionary crises. However, it could be beneficial to the classification method, once such operator is a kind of diversity generator operator. The solution found can then be compared to other sort of evolvable classifiers.

A. Training Process

The following algorithm is a possible implementation of the training process of the objective dialectical classifier:

- 1) Set the following initial parameters:
 - a) Number of historical phases, n_P ;
 - b) Length of each historical phase, n_H ;
 - c) Desired final number of poles, $n_{C,f}$;
 - d) Step of each historical phase, $0 < \eta(0) < 1$;
 - e) Maximum crisis, $0 \leq \chi_{\max} \leq 1$;
 - f) Initial number of poles $\#\Omega(0) = n_C(0)$, defining the initial set of poles:

$$\Omega(0) = \{C_1(0), C_2(0), \dots, C_{n_C(0)}(0)\}.$$

- 2) Set the following thresholds:
 - a) Minimum force, $0 \leq f_{\min} \leq 1$;
 - b) Minimum contradiction, $0 \leq \delta_{\min} \leq 1$;

- 3) Initialize the weights $w_{i,j}(0)$, where $1 \leq i \leq n_C(0)$ and $1 \leq j \leq n$.
- 4) Let $\#\Omega(t)$ be the cardinality of $\Omega(t)$, repeat until n_P iterations or $\#\Omega(t) = n_{C,f}$:

a) Repeat until n_H iterations:

- i) Initialize the measures of force $f_i = 0$, for $1 \leq i \leq n_C(t)$.
- ii) For all vectors of conditions

$$\mathbf{x} = (x_1, x_2, \dots, x_n)^T$$

of the input set $\Psi = \{\mathbf{x}^{(l)}\}_{l=1}^L$, repeat:

- A) Compute the values of the anticontradiction functions:

$$g_i(\mathbf{x}) = e^{-\|\mathbf{x} - \mathbf{w}_i\|},$$

where $1 \leq i \leq n_C(t)$.

- B) Calculate g_{\max} :

$$g_{\max} = \max\{g_1(\mathbf{x}), g_2(\mathbf{x}), \dots, g_{n_C(t)}(\mathbf{x})\}.$$

- C) Calculate the index $k(t)$ of the winner class:

$$g_i = g_{\max} \Rightarrow k(t) = i.$$

- D) Adjust the weights of the winner pole:

$$w_{i,j}(t+1) = \begin{cases} w'_{i,j}(t), & i = k(t) \\ w_{i,j}(t), & i \neq k(t) \end{cases},$$

where

$$w'_{i,j}(t) = w_{i,j}(t) + \eta(t)(x_j(t) - w_{i,j}(t)).$$

- E) Update the measure of force of the integrating poles:

$$f_i(t+1) = \begin{cases} f_i(t) + 1, & i = k(t) \\ f_i(t), & i \neq k(t) \end{cases}.$$

- iii) Quantitative changing: $\Omega(t+1) = \Omega(t)$.

- b) Calculate the normalized measures of force:

$$\bar{f}_i(t) = \frac{f_i(t)}{\max\{f_j(t)\}_{j=1}^{n_C(t)}},$$

for $1 \leq i \leq n_C(t)$.

- c) Compute the contradictions:

$$\delta_{i,j} = 1 - g_i(\mathbf{w}_j),$$

where $2 \leq j \leq n_C(t)$, $1 \leq i < j$, and find the maximum contradiction

$$\delta_{\max} = \max\{\delta_{i,j}, i \neq j\},$$

for $j = 2, 3, \dots, n_C(t)$ and $i = 1, 2, \dots, j-1$.

- d) Qualitative changing: compute the new set of poles, $\Omega(t+1)$:

$$\bar{f}_i(t) > f_{\min} \Rightarrow C_i(t) \in \Omega(t+1),$$

where $1 \leq i \leq n_C(t)$ and

$$\delta_{i,j} \geq \delta_{\min} \Rightarrow C_i(t), C_j(t) \in \Omega(t+1),$$

$$\delta_{i,j} < \delta_{\min} \Rightarrow C_i(t) \in \Omega(t+1),$$

$$\delta_{i,j} = \delta_{\max} \Rightarrow C_q \in \Omega(t+1),$$

where $2 \leq j \leq n_C(t)$, $1 \leq i < j$, $q = n_C(t) + 1$, and

$$\mathbf{w}_q = \frac{1}{2}(\mathbf{w}_i + \mathbf{w}_j).$$

- e) Add the crisis effect to the weights of the new integrating poles of the dialectical system:

$$w_{i,j}(t+2) = w_{i,j}(t+1) + \chi_{\max} G(0, 1),$$

for $1 \leq i \leq n_C(t+1)$, $1 \leq j \leq n$ and $\Omega(t+2) = \Omega(t+1)$.

B. Classification

Once the training process is complete, objective dialectical classifier behavior occurs in the same way as any non-supervised classification method. This is clear if we analyze the training process when $n_P = n_H = 1$. This transforms the ODC into a k-means method, for instance.

The classification is performed in the following way: given a set of input conditions

$$\mathbf{x} = (x_1, x_2, \dots, x_n)^T,$$

if the dialectical system reaches stabilization when $\Omega = \{C_1, C_2, \dots, C_{n_C}\}$, then we calculate:

$$g_{\max} = \max\{g_1(\mathbf{x}), g_2(\mathbf{x}), \dots, g_{n_C}(\mathbf{x})\}.$$

Therefore, the classification rule is:

$$g_k(\mathbf{x}) = g_{\max} \Rightarrow \mathbf{x} \in C_k,$$

where $1 \leq k \leq n_C$.

IV. CLASSIFICATION OF DW-MR MULTISPECTRAL IMAGES

A. Materials and Methods

The diffusion-weighted (DW) magnetic resonance (MR) images were acquired from the clinical images database of the Laboratory of MR Images, at the Physics Department of Universidade Federal de Pernambuco, Recife, Brazil. The database consists of real clinical images acquired from a clinical MR tomographer of 1.5 T. The MR images used in this work are those of a single volunteer with Alzheimer's. As a case study, three diffusion-weighted cerebral MR images were used of a 70-year-old male patient with Alzheimer's disease, with the following diffusion exponents: 0 s/mm², 500 s/mm² and 1000 s/mm², shown in the Figures 1, 2 and 3, respectively.

We selected MR images corresponding to slices showing the lateral ventriculi temporal corni in order to facilitate evaluations by the specialist, and correlations between data generated by the computational tool and the *a priori* knowledge of the specialist.

An image can be considered as a mathematical function, where its domain is a region of the plane of the integers, called *grid*, and its counterdomain is the set of the possible

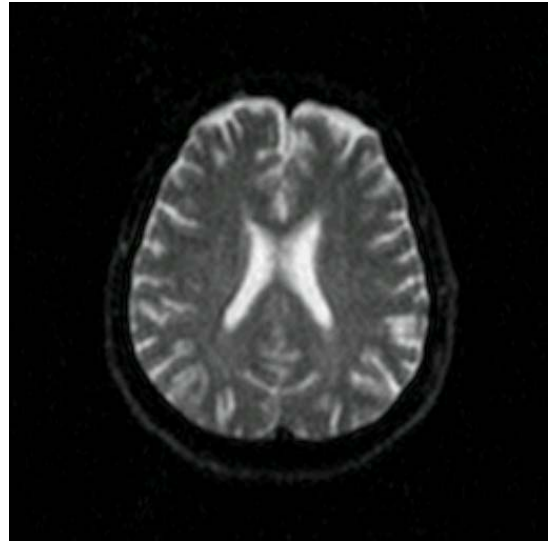


Fig. 1. Axial diffusion-weighted image with exponent diffusion of 0 s/mm²

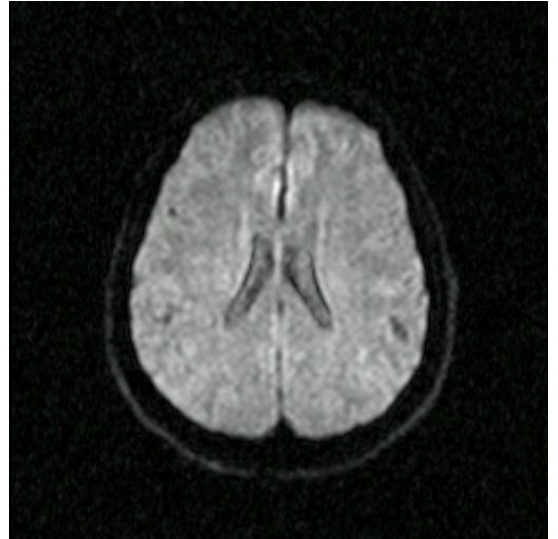


Fig. 2. Axial diffusion-weighted image with exponent diffusion of 500 s/mm²

values occupied by the pixels corresponding to each position on the grid.

Let $f_i : S \rightarrow W$ be the set of the diffusion-weighted MR images, where $1 \leq i \leq 3$, $S \subseteq \mathbf{Z}^2$ is the grid of the image f_i , where $W \subseteq \mathbf{R}$ is its counterdomain. The synthetic multispectral image $f : S \rightarrow W^3$ consisting of the MR images of the Figures 1, 2 and 3 is given by:

$$f(\mathbf{u}) = (f_1(\mathbf{u}), f_2(\mathbf{u}), f_3(\mathbf{u}))^T, \quad (1)$$

where $\mathbf{u} \in S$ is the position of the pixel in the image f , and f_1 , f_2 and f_3 are the diffusion-weighted MR images with diffusion exponents of $b_1 = 0$ s/mm², $b_2 = 500$ s/mm², and $b_3 = 1000$ s/mm², respectively.

The analysis of diffusion-weighted MR images is often performed using the resulting ADC map. Considering that each pixel $f_i(\mathbf{u})$ is approximately proportional to the signal

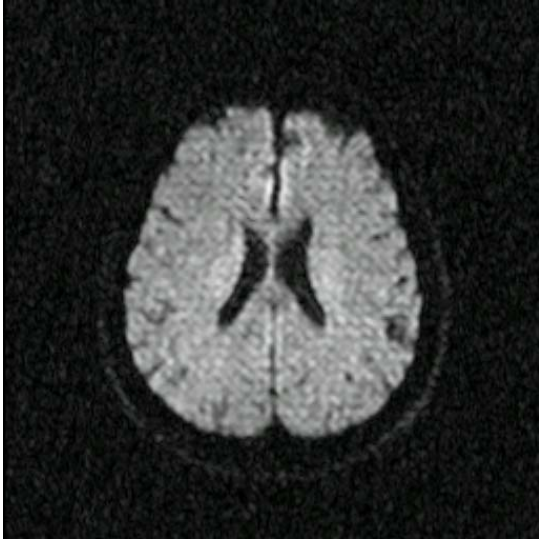


Fig. 3. Axial diffusion-weighted image with exponent diffusion of 1000 s/mm²

of the corresponding voxel as follows:

$$f_i(\mathbf{u}) = K\rho(\mathbf{u})e^{-T_E/T_2(\mathbf{u})}e^{-b_i D_i(\mathbf{u})}, \quad (2)$$

where $D_i(\mathbf{u})$ is the diffusion coefficient associated with the voxel mapped in the pixel in the position \mathbf{u} , $\rho(\mathbf{u})$ is the nuclear spin density in the voxel, K is a constant of proportionality, $T_2(\mathbf{u})$ is the transversal relaxation in the voxel, T_E is the echo time and b_i is the diffusion exponent, given by [15], [21]:

$$b_i = \gamma^2 G_i^2 T_E^3 / 3, \quad (3)$$

where γ is the gyromagnetic ratio and G_i is the gradient applied during the experiment i ; the ADC map $f_{\text{ADC}} : S \rightarrow W$ is calculated as follows:

$$f_{\text{ADC}}(\mathbf{u}) = \frac{C}{b_2} \ln \left(\frac{f_1(\mathbf{u})}{f_2(\mathbf{u})} \right) + \frac{C}{b_3} \ln \left(\frac{f_1(\mathbf{u})}{f_3(\mathbf{u})} \right), \quad (4)$$

where C is a constant of proportionality. Thus, the ADC map is given by:

$$f_{\text{ADC}}(\mathbf{u}) = CD(\mathbf{u}). \quad (5)$$

Therefore, the pixels of the ADC map are proportional to the diffusion coefficients in the corresponding voxels. However, as the images are acquired at different moments, the occurrence of noise in all the experiments must be considered. Furthermore, the presence of noise is amplified by the use of the logarithm.

Such factors lead us to the following conclusion: the pixels of the ADC map do not necessarily correspond to the diffusion coefficients because, for example, several pixels indicate high diffusion rates in voxels where the sample is not present, or in very solid areas like bone in the cranial box, as can be seen in Figure 4. This is the reason why such a map indicates *apparent* diffusion coefficients rather than *real* diffusion coefficients.

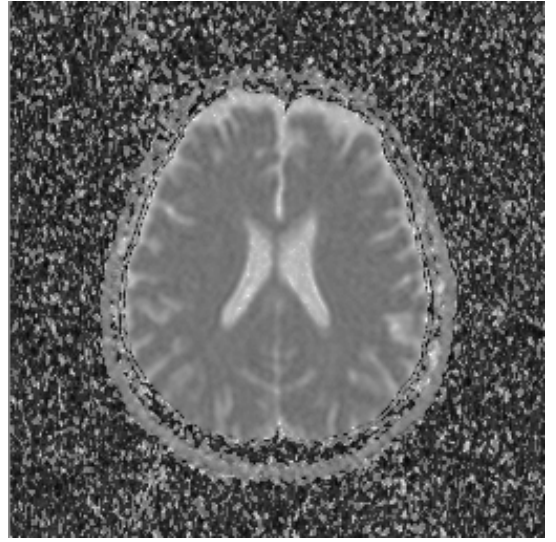


Fig. 4. ADC map calculated from the three diffusion images

In this paper we propose an alternative to the analysis of the ADC map: the multispectral analysis of the image $f : S \rightarrow W^3$ using the objective dialectical classifier.

Let the universe of classes of interest be defined as $\Omega = \{C_1, C_2, C_3\}$, C_1 represents the cerebrospinal fluid; C_2 , the white and the gray matter, as they cannot be distinguished using diffusion images, because their diffusion coefficients are very similar; and C_3 corresponds to the image background.

For the multispectral analysis using neural nets, the inputs are associated with the vector $\mathbf{x} = (x_1, x_2, x_3)^T$, where $x_i = f_i(\mathbf{u})$, for $1 \leq i \leq 3$. The net outputs represent the classes of interest and are associated with the vector $\mathbf{y} = (y_1, y_2, y_3)^T$, where each output corresponds to the class with the same index. The decision criterion employed in this analysis was the Bayes criterion: the output with greater value indicates the most probable class [22], [23], [24]. The training set and the test set were built using specialist knowledge during the selection of the regions of interest [25]. The synthetic multispectral image was classified using the following methods:

- 1) *Kohonen Self-Organized Map (SOM) classifier*: 3 inputs, 3 outputs, maximum of 200 iterations, initial learning rate $\eta_0 = 0.1$, circular architecture, Gaussian function of distance;
- 2) *Fuzzy c-means classifier*: 3 inputs, 3 outputs, maximum of 200 iterations, initial learning rate $\eta_0 = 0.1$;
- 3) *Radial Basis Function (RBF) network*: layer 1: a k-means clustering map with 3 inputs, 18 outputs, maximum of 200 iterations, initial learning rate $\eta_0 = 0.1$; layer 2: an one-layer perceptron with 18 inputs, 3 outputs, 75 iterations, training error of 5%, initial learning rate $\eta_0 = 0.1$.

To make comparisons between the proposed multispectral approach and the ADC map, we performed a monospectral non-supervised classification of the ADC map using a clustering-based method [26], [27]. We chose a Kohonen

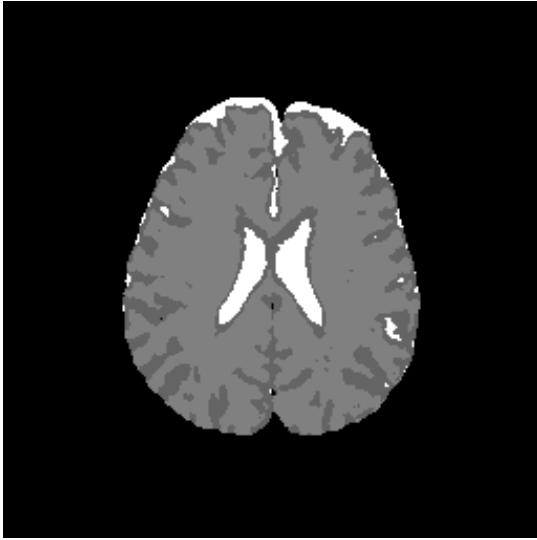


Fig. 5. Ground-truth image

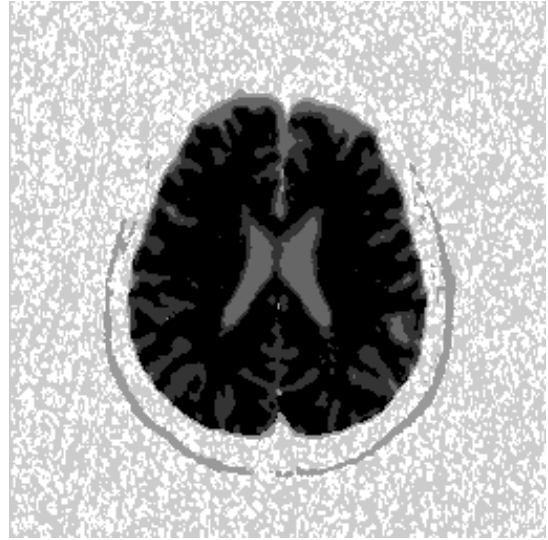


Fig. 6. Classification result by ODC before manual post-rotation

SOM classifier (KO-ADC) with 3 inputs, 3 outputs, maximum of 200 iterations, and initial learning rate $\eta_0 = 0.1$.

These methods were chosen in order to evaluate the behavior and performance of a classical neural network (RBF network) and well-known clustering-based networks (Kohonen SOM and fuzzy c-means) executing the task of classification of the synthetic multispectral image. Their initial learning rates and number of iterations were empirically determined.

B. Results

The ground-truth image was built by the use of a two-degree polynomial network to classify the multispectral image. The training set was assembled using anatomic information obtained from T_1 , T_2 and spin density MR images.

The ODC was trained using an initial system of 10 integrating classes, affected by 3 input conditions, studied during 5 historical 100-length phases, with an initial historical step $\eta_0 = 0, 1$. At the stages of revolutionary crisis we considered a minimum measure of force of 1%, minimum contradiction of 25 % and maximum crisis of 25%. The stop criterion was the final number of classes, in our case, 4 classes. The input conditions are the values of pixels on each of the 3 bands.

ODC training resulted in 6 classes, reduced to 4 classes after a manual post-rotation that merged the 3 classes external to the cranium, i.e. background, noise and cranial box, into a single class, namely background. This post-rotation was performed manually because the 3 populations are statistically different and only conceptually can they be reunited in a unique class. Figures 6 and 7 show the resulting classification by ODC before and after manual post-rotation, respectively.

From Figure 7 we can see that ODC was able to make a distinction between white and gray matter, the latter present in the interface between cerebrospinal fluid and white matter. Notice Figure 8, where an increased damaged area is

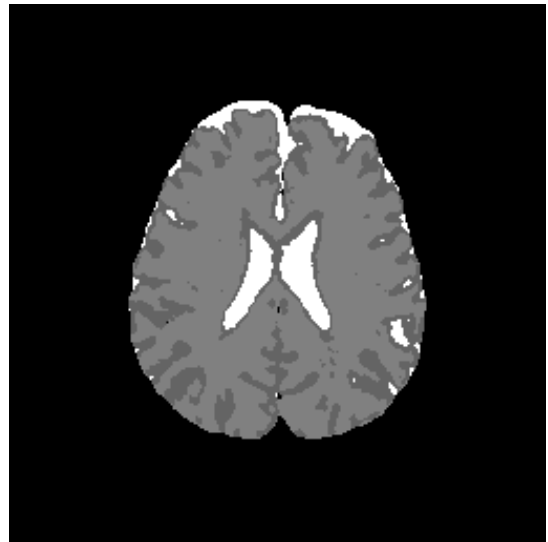


Fig. 7. Classification result by ODC after manual post-rotation. White areas are indication of cerebrospinal fluid, once gray and dark gray areas indicate white and gray matter, respectively.

highlighted. The classification fidelity was measured using the morphological similarity index, with structure element square 3×3 , and Wang's index [28], yielding 0.9877 and 0.9841, respectively.

Figures 9, 10, and 11 show classification results obtained by the use of classifiers based on Kohonen SOM (KO), RBF networks (RBF), and fuzzy c-means (CM), respectively, considering a fixed number of classes (white and gray matter, cerebrospinal fluid and background) [29], [30], [31], [32], [33]. Figure 12 shows the result of the classification of the ADC map using the Kohonen SOM classifier (KO-ADC) [33]. However, these visual results are evidence that, using such an approach, it is not possible to distinguish between white and gray matter in multispectral DW-MR Alzheimer's images.

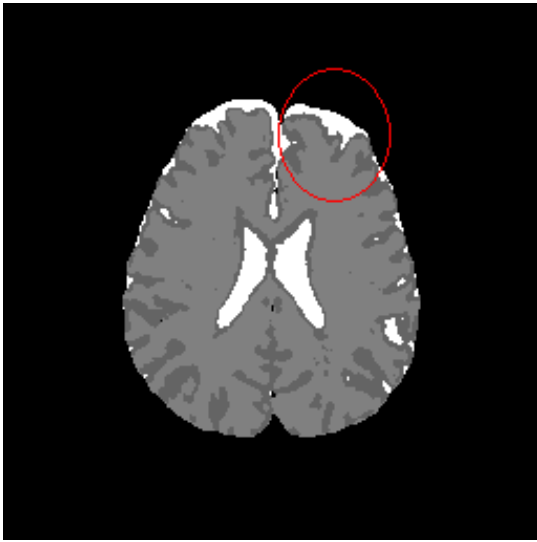


Fig. 8. Distinction between white and gray matter, emphasizing the damaged area

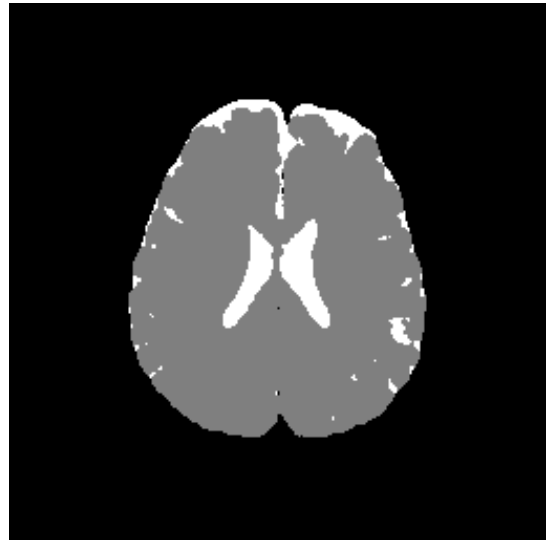


Fig. 10. Classification result by the RBF network classifier

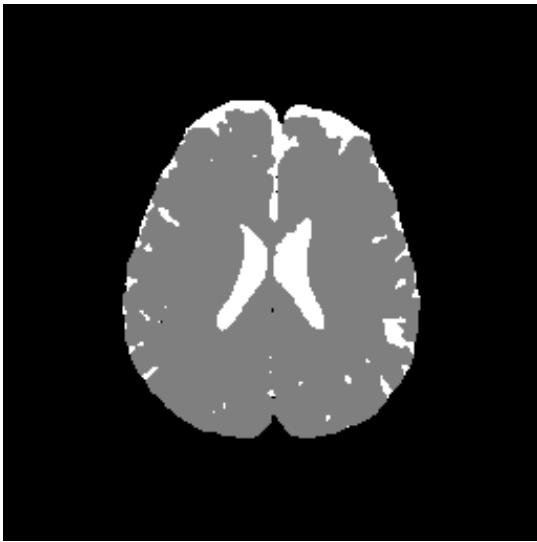


Fig. 9. Classification result by Kohonen SOM after manual post-rotation

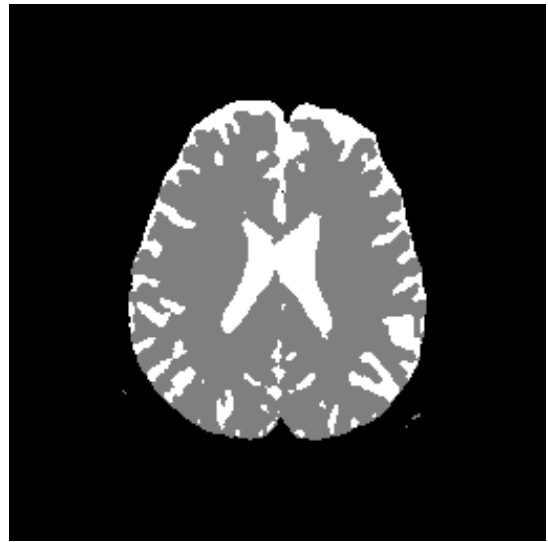


Fig. 11. Classification result by fuzzy c-means after manual post-rotation

V. CONCLUSIONS

The objective dialectical classifier is able to identify statistically significant classes in situations where the initial number of classes is not well known. It makes possible the detection of relevant classes and even singularities beyond the initial prediction. It can also aid the specialist to measure the volumes of interest, in an attempt to establish a correlation of such measuring with the advance of neurodegenerative diseases, such as Alzheimer's, and to distinguish significant alterations in the values of the measured diffusion coefficients. ODC can qualitatively and quantitatively improve the analysis of the human specialist.

In summary, the objective dialectical classifier can be used in problems where the number of statistically significant classes is not well known, or in problems where we need

to find a sub-optimum clustering map to be used for classification. The task of finding a suboptimum clustering map is empirical, as it is necessary to analyze the behavior of the training process as a function of the several parameters of the method, namely the minimum force, the minimum contradiction, the initial number of classes, the number of historical phases, the duration and the historical step of each historical phase. However, it is important to emphasize that, as the number of initial parameters is given, the classification performance of the dialectical classifiers is highly dependent on such initial parameters.

The objective dialectical method inaugurates a new family of evolvable methods inspired in the Philosophy, especially the Philosophy of Praxis, which can be used to solve both classical and new problems, such as the one presented in our case study.

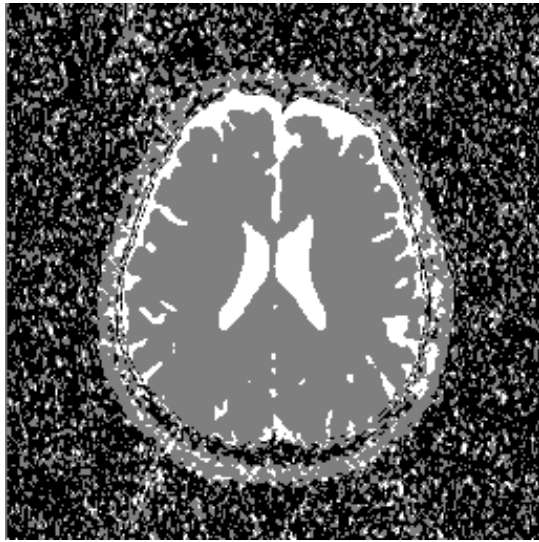


Fig. 12. Classification of ADC map by Kohonen SOM

We conclude by stating that philosophical thought is a great source of inspiration for constructing new computational intelligent methods, since we are simply returning to our original source of knowledge: Philosophy as a tool to a better understanding of nature and ourselves.

REFERENCES

- [1] K. Marx. Critique of Hegel's dialectics and philosophy. In *Economic and Philosophic Manuscripts of 1844*. International Publishers, 1980.
- [2] F. Engels. The role played by labor in the transition from ape to man. In *Collected Works of Karl Marx and Frederik Engels*. International Publishers, 1975.
- [3] A. Gramsci. Introduction to the Study of Philosophy and Historical Materialism. In *Prison Notebooks*. Columbia University, 1992.
- [4] A. Gramsci. Some Problems in the Study of the Philosophy of Praxis. In *Prison Notebooks*. Columbia University, 1992.
- [5] N. Bobbio. *Saggi su Gramsci*. Feltrinelli, Milano, 1990.
- [6] C. Thornley and F. Gibb. A dialectical approach to information retrieval. *Journal of Documentation*, 63(5):755–764, 2007.
- [7] J. B. Rosser Jr. Aspects of dialectics and nonlinear dynamics. *Cambridge Journal of Economics*, 24(3):311–324, 2000.
- [8] E. Engelhardt, D. M. Moreira, J. Lacks, V. M. Marinho, M. Rozenthal, and A. C. Oliveira Júnior. Doença de Alzheimer e espectroscopia por ressonância magnética do hipocampo. *Arquivos de Neuropsiquiatria*, 59(4):865–870, 2001.
- [9] M. Ewers, S. J. Teipel, O. Dietrich, S. O. Schönberg, F. Jessen, R. Heun, P. Scheltens, L. van de Pol, N. R. Freymann, H. J. Moeller, and H. Hampela. Multicenter assessment of reliability of cranial MRI. *Neurobiology of Aging*, (27):1051–1059, 2006.
- [10] M. S. Mega, I. D. Dinov, J. C. Mazziotta, M. Manese, P. M. Thompson, C. Lindshield, J. Moussai, N. Tran, K. Olsen, C. I. Zoumalan, R. P. Woods, and A. W. Toga. Automated brain tissue assessment in the elderly and demented population: Construction and validation of a sub-volume probabilistic brain atlas. *NeuroImage*, (26):1009–1018, 2005.
- [11] S. Xie, J. X. Xiao, J. Bai, and X. X. Jiang. Patterns of brain activation in patients with mild Alzheimer's disease during performance of subtraction: An fMRI study. *Clinical Imaging*, (29):94–97, 2005.
- [12] O. Naggara, C. Oppenheim, D. Rieu, N. Raoux, S. Rodrigo, G. D. Barba, and J. F. Meder. Diffusion tensor imaging in early Alzheimer's disease. *Psychiatry Research Neuroimaging*, (146):243–249, 2006.
- [13] M. Bozzali, A. Falini, M. Franceschi, M. Cercignani, M. Zuffi, G. Scotti, G. Comi, and M. Filippi. White matter damage in alzheimer's disease assessed in vivo using diffusion tensor magnetic resonance imaging. *Journal of Neurology, Neurosurgery and Psychiatry*, 72:742–746, 2002.
- [14] A. T. Du, N. Schuff, L. L. Chao, J. Kornak, F. Ezekiel, W. J. Jagust, J. H. Kramer, B. R. Reed, B. L. Miller, D. Norman, H. C. Chui, and M. W. Weiner. White matter lesions are associated with cortical atrophy more than entorhinal and hippocampal atrophy. *Neurobiology of Aging*, (26):553–559, 2005.
- [15] E. M. Haacke, R. W. Brown, M. R. Thompson, and R. Venkatesan. *Magnetic Resonance Imaging: Physical Principles and Sequence Design*. Wiley-Liss, 1999.
- [16] R. L. Marchetti, C. M. C. Bottino, D. Azevedo, S. K. Nagahashi-Marie, and C. C. Castro. Confiabilidade de medidas volumétricas de estruturas temporais mesiais. *Arquivos de Neuropsiquiatria*, 60(2B):420–428, 2002.
- [17] O. T. Carmichael, H. A. Aizenstein, S. W. Davis, J. T. Becker, P. M. Thompson, C. C. Meltzer, and Y. Liu. Atlas-based hippocampus segmentation in Alzheimer's disease and mild cognitive impairment. *NeuroImage*, (27):979–990, 2005.
- [18] Y. Hirata, H. Matsuda, K. Nemoto, T. Ohnishi, K. Hirao, F. Yamashita, T. Asada, S. Iwabuchi, and H. Samejima. Voxel-based morphometry to discriminate early Alzheimer's disease from controls. *Neuroscience Letters*, (382):269–274, 2005.
- [19] N. Pannacciulli, A. Del Parigi, K. Chen, D. S. N. T. Le, E. M. Reiman, and P. A. Tataranni. Brain abnormalities in human obesity: A voxel-based morphometric study. *NeuroImage*, (31):1419–1425, 2006.
- [20] S. Hayasaka, A. T. Du, A. Duarte, J. Kornak, G. H. Jahng, M. W. Weiner, and N. Schuff. A non-parametric approach for co-analysis of multi-modal brain imaging data: Application to Alzheimer's disease. *NeuroImage*, (30):768–779, 2006.
- [21] Z. P. Liang and P. C. Lauterbur. *Principles of Magnetic Resonance Imaging: A Signal Processing Perspective*. IEEE Press, New York, 2000.
- [22] R. Duda, P. Hart, and D. G. Stork. *Pattern Classification*. John Wiley and Sons, 2001.
- [23] R. Duda and P. Hart. *Pattern Classification and Scene Analysis*. John Wiley and Sons, 1972.
- [24] J. Sklansky and G. N. Wassel. *Pattern Classifiers and Trainable Machines*. Springer-Verlag, 1st edition, 1981.
- [25] S. Haykin. *Neural Networks: A Comprehensive Foundation*. Prentice Hall, New York, 1999.
- [26] H. Li, T. Liu, G. Young, L. Guo, and S. T. C Wong. Brain Tissue Segmentation Based on DWI/DTI Data. In *Proceedings of the ISBI 2006*. CS-IEEE, 2006.
- [27] A. Bartsaghi and M. Nadar. Segmentation of Anatomical Structure from DT-MRI. In *Proceedings of the ISBI 2006*. CS-IEEE, 2006.
- [28] Z. Wang and A. C. Bovik. A universal image quality index. *IEEE Signal Processing Letters*, 9, 2002.
- [29] W. P. Santos, R. E. Souza, A. F. D. Silva, and P. B. Santos Filho. Evaluation of Alzheimer's disease by analysis of MR images using multilayer perceptrons and committee machines. *Computerized Medical Imaging and Graphics*, 32(1):17–21, 2008.
- [30] W. P. Santos, R. E. Souza, A. F. D. Silva, and P. B. Santos Filho. Evaluation of Alzheimer's disease by analysis of MR images using multilayer perceptrons, polynomial nets and Kohonen LVQ classifiers. In *Lecture Notes in Computer Science: Computer Vision / Computer Graphics Collaboration Techniques and Applications (MIRAGE 2007)*, volume 2, pages 12–22, Rocquencourt, France, 2007. INRIA & CS-IEEE.
- [31] W. P. Santos, R. E. Souza, A. F. D. Silva, and P. B. Santos Filho. Avaliação da Doença de Alzheimer pela Análise Multiespectral de Imagens DW-MR por Mapas Auto-Organizados de Kohonen como Alternativa aos Mapas ADC. In *IV Congresso Latino-Americano de Engenharia Biomédica*, Porlamar, Venezuela, 2007. IFMBE.
- [32] W. P. Santos, R. E. Souza, A. F. D. Silva, and P. B. Santos Filho. Avaliação da doença de Alzheimer pela análise multiespectral de imagens DW-MR por redes RBF como alternativa aos mapas ADC. In *VIII Congresso Brasileiro de Redes Neurais*, Florianópolis, Brasil, 2007. SBRN.
- [33] W. P. Santos, R. E. Souza, and P. B. Santos Filho. Evaluation of Alzheimer's disease by analysis of MR images using multilayer perceptrons and Kohonen SOM classifiers as an alternative to the ADC maps. In *29th Annual International Conference of the IEEE Engineering in Medicine and Biology Society*, Lyon, France, 2007. EMBS-IEEE.